The Hippo signaling pathway effector YAP promotes salivary gland regeneration after injury

Rocchi, Cecilia; Cinat, Davide; Serrano Martinez, Paola; Jellema-de Bruin, Anne L.; Baanstra, Mirjam; Brouwer, Uilke; Del Angel Zuivre, Cinthya; Schepers, Hein; van Os, Ronald; Barazzuol, Lara

Published in:
Science signaling

DOI:
10.1126/scisignal.abk0599

REGENERATION

The Hippo signaling pathway effector YAP promotes salivary gland regeneration after injury

Cecilia Rocchi[1,2]†, Davide Cinat[1,2]‡, Paola Serrano Martinez[1,2]‡§, Anne L. Jellema-de Bruin[1,2], Mirjam Baanstra[1,2], Uilke Brouwer[1,2], Cinthya del Angel Zuivre[1], Hein Schepers[1], Ronald van Os[3], Lara Barazzuol[1,2]*, Robert P. Coppes[1,2]*

Salivary glands are damaged by radiotherapy for head and neck cancers, which often culminates in radiation-induced hyposalivation and xerostomia that may be permanent. Here, we identified a central role for YAP in the regenerative response of the salivary gland. Activation of the Hippo signaling pathway inhibits the phosphorylation of YAP, leading to its nuclear translocation and transcriptional activity. Using mice with salivary gland injury induced by surgical ligation and salivary gland–derived organoids, we found that YAP nuclear localization in the salivary gland epithelium changed dynamically between homeostasis and regeneration. Whereas local injury had no effect on nuclear YAP localization in saliva-producing acinar cells, it triggered nuclear accumulation of YAP in saliva-transporting ductal cells. Injury also stimulated the proliferation of ductal cells, which were mainly quiescent under homeostatic conditions and in nonregenerating areas distal to the injury site, thus enabling salivary gland regeneration. Overexpressing YAP or driving YAP nuclear translocation by inhibiting upstream Hippo pathway kinases increased the capacity of mouse and human salivary gland cells, including human cells that had been irradiated, to form lobed organoids in vitro. Our results identify a YAP-driven regeneration program in salivary gland ductal cells that could be used to promote salivary gland regeneration after irradiation-induced damage.

INTRODUCTION

Radiotherapy is a major part of the treatment for more than 500,000 patients who are annually diagnosed with head and neck cancer worldwide (*1*). Although radiotherapy treatment substantially increases the survival rate of these patients, the unavoidable inclusion of healthy salivary glands within the radiation field leads to a high probability of developing late radiation toxicity that culminates in radiation-induced hyposalivation and xerostomia (*2*–*4*). The extent of structural damage and subsequent functional decline of an organ after radiation treatment depends on the cellular radiosensitivity of the given tissue (*4*). The salivary gland epithelium is composed of morphologically and functionally distinct epithelial cell types and compartments: the secretory acinar cells that are responsible for the production of saliva and a network of branched ductal cells that transport the saliva to the oral cavity (*5*). Similar to other adult tissue, such as the intestine (*6*), different compartments of the gland display differential responses to ionizing radiation both in terms of kinetics and sensitivity (*7*).

The acinar compartment, the functional secretory unit of the salivary gland, has been shown to be mitotically active, thus playing an important role in the maintenance of adult mouse salivary gland tissue homeostasis (*8*, *9*). In addition, upon radiation damage, acinar cells positive for the pluripotency-associated transcription factor SRY-box transciptor factor 2 (SOX2) show regenerative capacity within the first 30 days after irradiation (*9*). Their regenerative capacity, however, appears to be limited, and their eventual loss of proliferative capacity due to radiation-induced damage leads to the loss of the functional acinar compartment (*7*, *9*, *10*). In contrast, cells of the excretory duct compartment, which comprises cells of the intercalated and striated ducts that modify the saliva composition, appear to be in a relatively quiescent state (*11*, *12*). The slow turnover of these cells and the observation that ductal cells show little to no loss of duct-specific marker expression after irradiation (*9*) may be indicative of a relative resistance to radiation-induced damage, similar to what has been observed for brain cells (*13*, *14*). Although some lineage-tracing studies in adult mouse salivary glands point toward the existence of mainly progenitor lineage-restricted populations marked by keratin 14 ($K14^+$) and either c-Kit (Kit) or keratin 5 ($K5^+$) within the ductal compartment (*10*, *15*), others point to possible plasticity within the intercalated and excretory duct compartments in contributing to the regeneration of functional acinar units in irradiated glands (*16*). However, after high radiation doses, these compartments fail to fully regenerate the salivary gland tissue, ultimately leading to the functional loss of saliva production (*16*–*18*).

We previously showed, in both rats and patients, that the radiation dose delivered to the region of the parotid salivary gland containing the main ducts predicts salivary gland dysfunction (*19*). This supports the idea of the existence of a stem/progenitor cell population residing in the main excretory ducts, and therefore, sparing this region has been proposed as a means to preserve saliva production after radiotherapy treatment (*19*, *20*). Furthermore, in vitro three-dimensional (3D) culture of salivary gland Wnt-responsive cells has demonstrated the competence of excretory ductal cells producing high amounts of epithelial cell adhesion molecule ($Epcam^{high}$ cells) to enter into the cell cycle and give rise to organoids containing terminally

[1]Department of Biomedical Sciences of Cells and Systems, University Medical Center Groningen, University of Groningen, Groningen 9713 AV, Netherlands. [2]Department of Radiation Oncology, University Medical Center Groningen, University of Groningen, Groningen 9700 RB, Netherlands. [3]European Research Institute for the Biology of Ageing, University Medical Center Groningen, University of Groningen, Groningen 9713 AV, Netherlands.
*Corresponding author. Email: r.p.coppes@umcg.nl (R.P.C); l.barazzuol@umcg.nl (L.B.)
†Present address: Centre for Regenerative Medicine, Institute for Regeneration and Repair, The University of Edinburgh, Edinburgh BioQuarter, 5 Little France Drive, Edinburgh, EH16 4UU, UK.
‡These authors contributed equally to this work.
§Present address: Ocular Angiogenesis Group, Departments of Ophthalmology and Medical Biology, Amsterdam University Medical Centers, University of Amsterdam, Amsterdam 1105 AZ, Netherlands.

differentiated acinar cells, indicating that the appropriate signaling stimulation can guide the quiescent compartment to an active state capable of generating a structure resembling that of the native tissue. Wnt signaling has been shown to drive in vitro self-renewal and maintenance of salivary glands, but the pathways involved in regeneration of the salivary glands after injury remain poorly understood.

The transcriptional regulator Yes-associated protein (YAP) has emerged as a key promoter of tissue growth and regeneration in various organs, including the intestine, liver, and skin (*21*, *22*). YAP transcriptional activity relies on changes in its nuclear-cytoplasmic localization that are tightly controlled by the Hippo pathway. The Hippo pathway consists of a highly conserved group of serine-threonine kinases that determine YAP cellular localization. The core kinases of the Hippo pathway are MST1 and MST2, which activate the kinases LATS1 and LATS2, causing them to phosphorylate YAP at Ser^{127}, leading to the retention of YAP in the cytoplasm. Inactivation of this kinase cascade leads to YAP nuclear translocation and binding to TEA domain (TEAD) family of transcription factors, thus stimulating the expression of target genes that promote cell growth and proliferation. The ectopic expression of *YAP* has been shown to promote stem/progenitor cell expansion and the dedifferentiation of somatic epithelial cells, such as those of the mammary gland and pancreas, to a stem cell state (*23*), opening important opportunities for exploiting YAP in regenerative medicine. The capacity to increase the stem cell number or transiently activate existing stem cells could be especially important in tissues with slow turnover or a low regenerative potential, such as the salivary gland (*22*, *24*). YAP function has been implicated in the development of the salivary gland. Deletion of *YAP* in the developing mouse salivary gland epithelium leads to severe morphogenesis defects of the glands, reflecting compromised epithelial patterning (*25*). The inability of *YAP*-null embryonic salivary gland epithelium to specify ductal progenitors indicates the importance of YAP during the development of salivary glands (*25*).

Here, we report an essential role for YAP-mediated transcriptional activity during homeostasis and regeneration of adult salivary glands after damage. In addition to having a pivotal role during salivary gland development (*25*), we show that YAP activity changes dynamically between homeostasis and regeneration in adult glands. Upon salivary gland ligation, YAP nuclear localization increased in the ductal compartment at the site of regeneration, supporting the existence of a relatively quiescent stem cell–like population residing in the striated ducts (*26*). Using a 3D organoid culture system that has been shown to mimic regeneration (*26*–*28*), we provide evidence that YAP inactivation diminished the organoid-forming capacity of stem/progenitor cells derived from mouse and human adult salivary glands, whereas YAP overexpression promoted stem/progenitor organoid culture expansion. We also demonstrated that induction of YAP nuclear translocation after irradiation promoted regeneration in vitro. Our data further support the idea that salivary gland regeneration after severe damage can be mediated by newly activated ductal cells and that stimulation of YAP nuclear translocation could be used to promote the regeneration of radiation-damaged salivary glands.

RESULTS

Nuclear YAP increases in salivary gland ductal cells during regeneration

We used an in vivo mouse injury model to investigate the potential role of YAP in control and regenerating adult salivary glands. Both submandibular glands were sutured below the sublingual glands to induce a dynamic regenerative response of the gland. The suture causes the division of the salivary gland into two distinct regions: a lower caudal region and an upper cranial region (Fig. 1A and fig. S1, A and B). To trace proliferating cells, the mice were subjected to two bromodeoxyuridine (BrdU) injections at 24 and 6 hours before sacrifice. Within 14 days of ligation, a loss of tissue morphology in the lower caudal region of the gland was evident (fig. S1, B and D). Immunofluorescence staining showed a pronounced reduction in $AQP5^+$ (aquaporin 5–positive) acinar cells in the lower caudal region of the gland, whereas the upper cranial region retained high AQP5 abundance, indicative of an intact and functional acinar cell compartment (fig. S1, C and D).

Given the pronounced damage that the suture induced to the lower caudal region of the gland, we investigated whether regeneration was taking place in the upper cranial region of the gland. A significant increase of $BrdU^+$ cells was observed in close proximity to the suture (the regeneration site) (Fig. 1B and fig. S1D) compared to the homeostatic area of the gland (distal to the regeneration site) and to the control gland. Whereas the control gland and the homeostatic area of the ligated gland predominantly showed proliferation activity in the intercalated duct and acinar compartments, at the regeneration site proliferation was predominantly in the excretory and striated ductal compartments. These differences in the regenerative response between the cranial and caudal regions of the gland are in accordance with the idea that the ductal compartment contributes to the regeneration of the gland (*19*).

Because YAP subcellular location determines its activity, we examined whether there were distinct patterns of YAP protein localization within the ligated submandibular gland and the control gland. Consecutive submandibular gland sections were analyzed by immunohistochemistry (IHC) for total YAP and BrdU. IHC analysis revealed that YAP was predominantly present in the acinar and intercalated ductal compartments in control salivary glands (Fig. 1B). The excretory ductal compartment, where quiescent stem/progenitor cells have been suggested to reside (*26*, *29*), showed a weak cytoplasmic localization of YAP. At 2 weeks after ligation, IHC for total YAP showed a markedly distinct distribution in the submandibular gland epithelium, with increased nuclear YAP in the excretory and striated ductal compartments at the regeneration site and a lower amount of nuclear YAP confined predominantly to the acinar intercalated duct compartment in the homeostatic area of the ligated gland (Fig. 1B and fig. S1E).

The BrdU and nuclear YAP patterns along the proximal-distal axis of the regeneration site indicated a potential dynamic role of YAP during regeneration of the injured gland. To confirm the role of YAP as sensor of tissue integrity in salivary gland and potential driver of the regeneration program, we assessed the regeneration potential of salivary glands upon inhibition of YAP activity using verteporfin (VP), which blocks the YAP-TEAD interaction. Ligated and control mice were treated with VP at several time points after suturing (Fig. 1C). To test whether salivary gland regeneration was impaired, at day 30 after suture, we evaluated the potential of salivary gland–derived cells to form organoids ex vivo as a surrogate readout of epithelial regeneration potential. Purified primary ductal cells isolated from the mouse submandibular glands were seeded in Matrigel and cultured as organoids as previously described (*26*, *27*). The organoid-forming efficiency (OFE) of cells derived from ligated, VP-treated glands was significantly reduced compared to that of cells

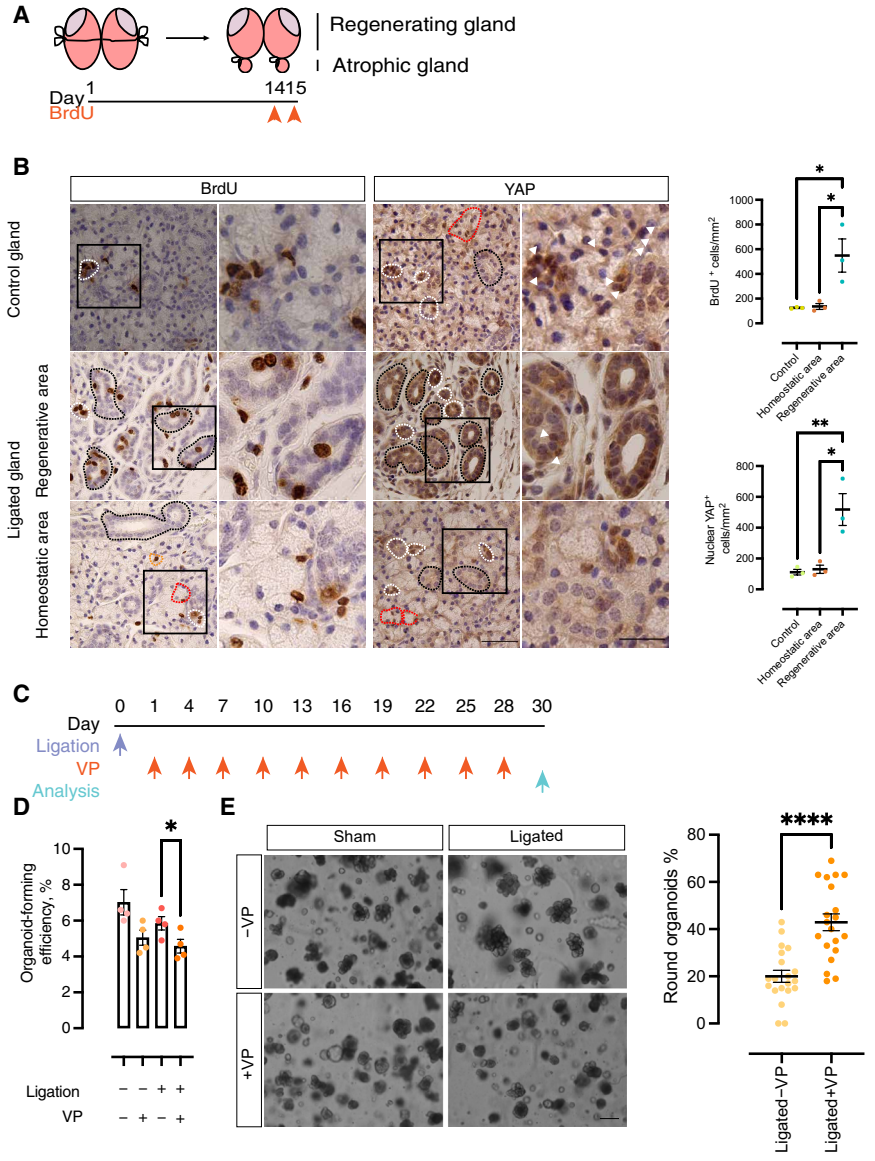

Fig. 1. YAP nuclear accumulation increases in the striated and excretory ductal compartment at the regenerative site of the submandibular gland. (**A**) Schematic showing the time course of the ligation injury model and BrdU pulses in adult mice. (**B**) Imaging and quantification of BrdU incorporation and nuclear YAP staining in control and ligated submandibular glands at 14 days after ligation. Intercalated ducts are outlined in white; striated and excretory ducts are outlined in black, and acinar cells are outlined in red. Scale bars, 50 μm. Cells with nuclear YAP localization are indicated by white arrowheads. $BrdU^+$ and nuclear YAP^+ cells per square millimeter of tissue were quantified in control homeostatic gland and in regenerative and homeostatic areas in ligated glands. $n = 3$ mice per condition. Data are represented as means ± SEM. Normal distribution was tested using the Shapiro-Wilk test. Statistical significance between the three groups was determined using one-way analysis of variance (ANOVA) followed by Tukey's multiple comparison test ($P < 0.05$). (**C**) Schematic showing the time course of verteporfin (VP) treatment in vivo. (**D**) Organoid forming efficiency of mouse salivary gland–derived cells isolated from mice treated with or without VP. $n = 4$ mice per treatment group. Normal distribution of the data was tested using Shapiro-Wilk test. Statistical significance between the groups was determined using one-way ANOVA followed by Tukey's multiple comparison test. Data are represented as means ± SEM. (**E**) Representative images of mouse salivary gland organoids derived from control and ligated glands in nontreated and VP-treated mice. The formation of round organoids derived from dissociated tissue samples was quantified for ligated glands from nontreated mice and for ligated glands from VP-treated mice. Shape of organoids was assessed from four independent experiments. Data are represented as means ± SEM. Normal distribution of the data was assessed using Shapiro-Wilk test. Statistical significance between the groups was determined using independent sample *t* test ($P < 0.05$). *$P < 0.05$, **$P < 0.01$, and ****$P < 0.0001$.

derived from ligated untreated glands (Fig. 1, D and E). We also observed a decrease in OFE of cells derived from nonligated VP-treated glands compared to nonligated and untreated glands, suggesting that an active YAP program is required for homeostatic maintenance in the adult submandibular gland. In vivo treatment with VP not only significantly reduced the OFE of salivary gland cells but also significantly increased the proportion of organoids that were round instead of lobular, indicating a potential role for YAP in branching morphogenesis (Fig. 1E), similar to what has been observed in embryonic salivary gland (*25*). Together, these results suggest that YAP plays a role in the initiation of damage-induced salivary gland regeneration.

YAP nuclear activity drives mouse salivary gland organoid growth

Given the increase in YAP nuclear localization in salivary gland ductal cells during regeneration in vivo, we investigated the function of YAP in the self-renewal potential of mouse salivary gland stem/progenitor cells (SGSPCs) as assessed in vitro by OFE. Before modulating YAP activity in the ex vivo salivary gland regeneration model, we assessed whether the tissue dissociation procedure that was used to isolate the cells altered the phosphorylation status of YAP and, therefore, its nuclear activity. Quantification of phosphorylated YAP (pYAP), the form that is sequestered in the cytoplasm, at different stages of the procedure showed an increase in pYAP during the dissociation process, suggesting a low activity of nuclear YAP in dissociated cells. This higher amount of pYAP measured at the single-cell stage before seeding into Matrigel confirmed that activation of the YAP-driven program was not induced by the dissociation procedure (fig. S2, A and B).

Impairment of YAP nuclear activity using VP treatment at the single-cell stage (day 0) completely abrogated organoid formation (Fig. 2, A and B), whereas drug exposure in 4-day-old organoids led to a collapse of the organoid structure and impairment to form secondary organoids in the next passage (Fig. 2, C and D, and fig. S2, C and D). Similarly, small interfering RNA (siRNA)–mediated *YAP* knockdown led to a significant decrease of salivary gland OFE

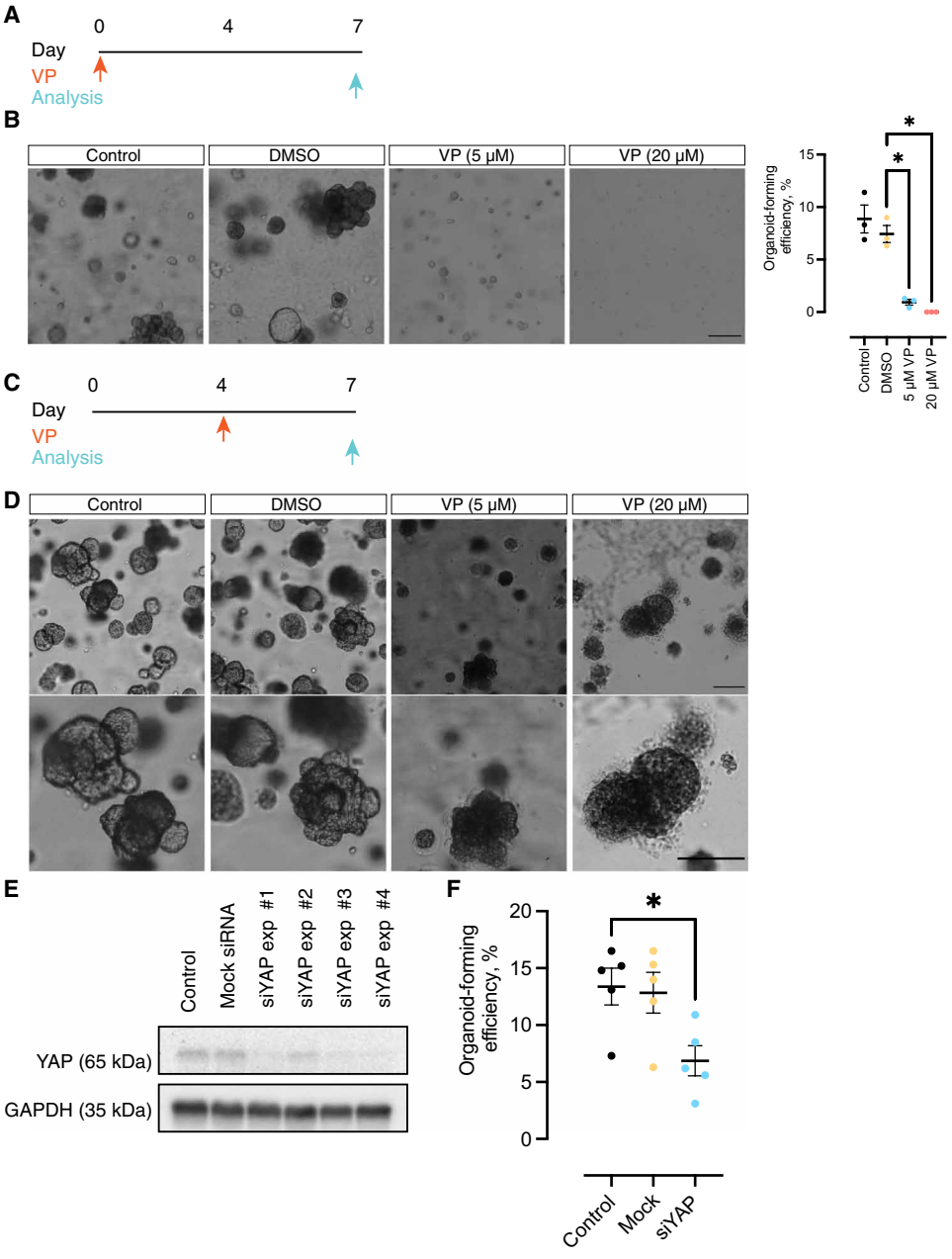

Fig. 2. Inhibition of YAP nuclear localization reduces self-renewal of adult mouse SGSPCs. (**A**) Salivary gland–derived cells were placed in organoid culture in the presence of VP and analyzed 7 days later. (**B**) Representative images and quantification of organoid formation efficiency for salivary gland cells that were nontreated (control) or treated with vehicle (DMSO) or VP (5 and 20 μM) from the start of the culture. Each dot represents a different mouse ($n = 3$). Data represent means ± SEM. Statistical significance between the groups was tested using one-way ANOVA followed by Tukey's multiple comparison test. Scale bar, 50 μm. (**C**) Salivary gland–derived cells were placed in organoid culture, treated with VP at day 4, and analyzed at day 7. (**D**) Representative images of mouse salivary gland cells after treatment with VP from day 4. (**E**) Western blot analysis for total YAP in mouse salivary gland organoids that were not transfected (control) or transfected with scrambled siRNA (mock) or siYAP (four different experiments, exp #1 to exp #4). (**F**) Organoid formation efficiency of salivary gland cells treated as in (E). Each dot represents a different mouse ($n = 5$). Data represent means ± SEM. Kruskal-Wallis test followed by Dunn's multiple comparison test was used to test the differences between the groups ($P < 0.05$). *$P < 0.05$.

(Fig. 2, E and F). These data suggest an essential role of YAP nuclear activity for SGSPC self-renewal and maintenance. We reasoned that if inhibition of YAP nuclear activity led to reduced OFE, enhanced YAP nuclear translocation could lead to increased self-renewal potential and expansion of SGSPCs. Treatment of salivary gland–derived single cells with lipophosphatidic acid (LPA) (Fig. 3A), a compound known to inhibit LATS1 and LATS2 kinase activity through the modification of cytoskeleton tension (*30*), led to decreased pYAP/YAP ratio (Fig. 3B), indicating that the increase in OFE upon LPA treatment is driven by increased YAP nuclear activity (Fig. 3, C and D). To further confirm the importance of YAP nuclear activity in SGSPC self-renewal, we performed siRNA-mediated knockdown of *LATS1*, which led to a decrease in pYAP (Fig. 3E) and an increase in OFE compared to controls (Fig. 3, F and G), further highlighting the importance of Hippo signaling in the activity of SGSPCs.

YAP overexpression in human salivary gland–derived organoids increases stem cell potential

To validate that increased YAP nuclear translocation increases the self-renewal capacity of SGSPCs, we investigated whether ectopic expression of YAP in human salivary gland organoid–derived cells would have similar effects as LPA treatment in mouse cells. Human salivary gland organoid-derived cells at the end of passage 1 (P1) were transduced with a lentiviral vector encoding fluorescently tagged wild-type YAP (pGAMA-YAP) (*31*). As a control, cells were transduced with an empty lentiviral vector (t2a-mCherry). Transduced cells were cultured for 7 days and, after isolation by fluorescence-activated cell sorting (FACS) for mCherry, plated in Matrigel to assess secondary organoid formation potential (Fig. 4A). YAP overexpression was confirmed by Western blot analysis of total YAP protein (Fig. 4B). YAP-overexpressing cells ($mCherry^{+}$ YAP^{OE}) cultured in enriched media (EM) gave rise to a significantly higher number of secondary organoids compared to mCherry-expressing cells (fig. S3A). This difference was maintained for the subsequent three passages (Fig. 4, C and D). We also found that the number of cells and the size of the

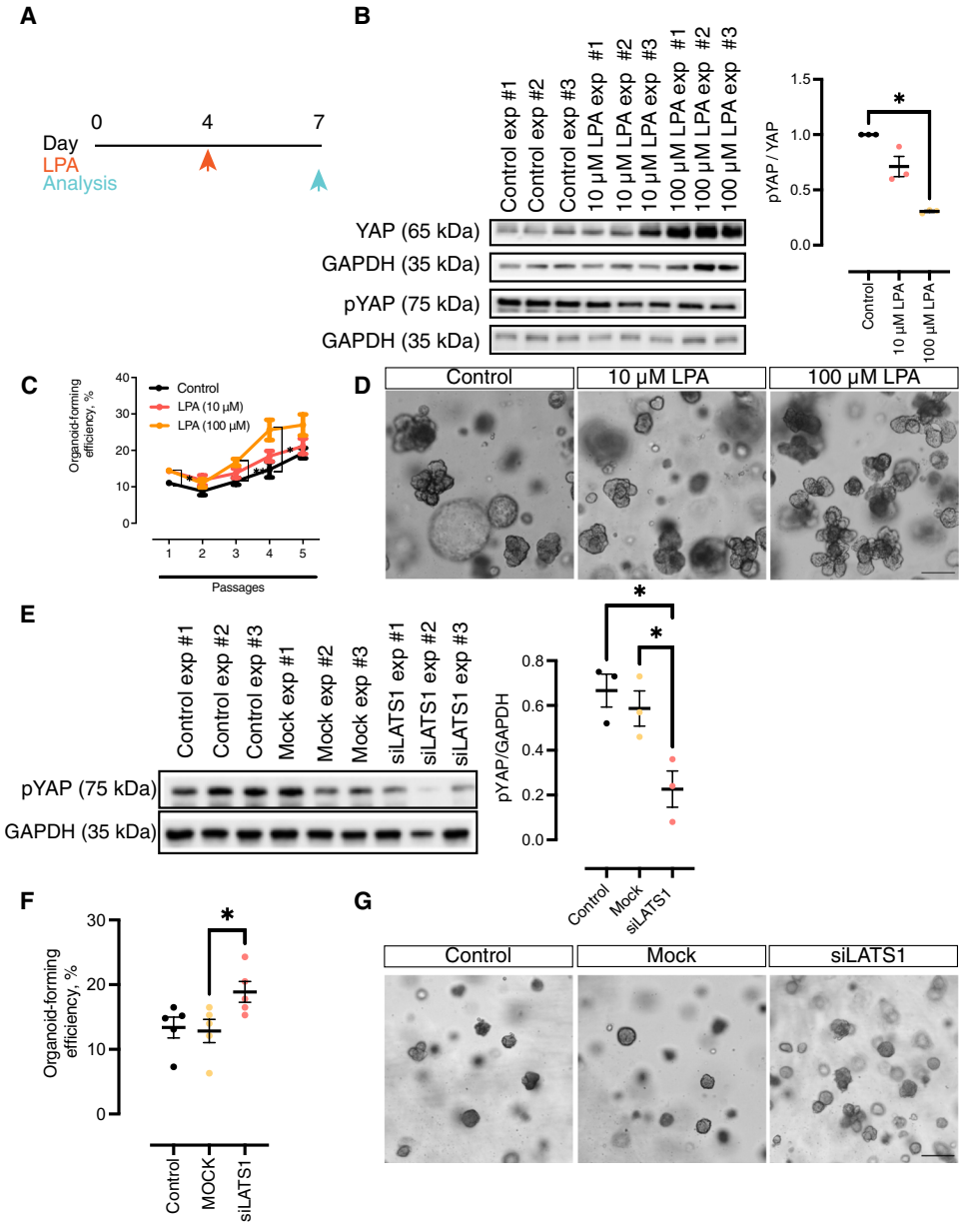

Fig. 3. Stimulation of YAP nuclear translocation increases the capacity of salivary gland cells to form organoids. (**A**) Schematic showing the timeline of LPA treatment in salivary gland–derived organoid culture. (**B**) Western blotting for and quantification of total and phosphorylated YAP (pYAP) in lysates from mouse salivary gland–derived organoids treated with or without 10 and 100 μM LPA. GAPDH is a loading control. $n = 3$ mice. Data are represented as means ± SEM. Kruskal-Wallis test followed by Dunn's multiple comparison test was used to test the differences between the groups ($P < 0.05$). (**C**) Organoid formation efficiency of mouse salivary gland–derived organoids treated with 10 or 100 μM LPA over five passages. Each dot represents a culture derived from a different mouse. $n = 6$. Two-way ANOVA followed by Tukey's test for multiple comparison was used to test the significance between the groups. (**D**) Representative images of LPA-treated mouse salivary gland organoids at the end of passage 5. Scale bar, 50 μm. (**E**) Western blot analysis and quantification of pYAP in mouse salivary gland organoids that were not transfected (control) or transfected with scrambled siRNA (Mock) or siLATS1 (three different experiments for each, exp #1 to exp #3). (**F**) Organoid formation by cells in (E). $n = 5$ cultures derived from different mice per condition. Data are represented as means ± SEM. One-way ANOVA followed by Tukey's test for multiple comparison was used to test significance between the groups. (**G**) Representative images of organoids derived from LATS-knockdown cells. Scale bar, 50 μm. *$P < 0.05$.

organoids were significantly increased in YAP^{OE} cells compared to controls (Fig. 4, E and F). We observed that the overexpression of YAP in human salivary gland–derived organoids cultured in Wnt-enriched media that also contains the Wnt signaling potentiator R-Spondin 1 (RSPO1), the transforming growth factor–β inhibitor A8301, and Noggin (WRYTN) did not support the expansion of the culture to the same extent as did EM, indicating that YAP and Wnt could have different roles or act at different times during the regeneration process (fig. S3, B and C). These results indicate that YAP overexpression promotes stem cell properties in human salivary gland–derived cells. Human salivary gland organoids overexpressing YAP and cultured in EM showed a branched morphology phenotype at the end of P1, which greatly differed from the round shape of non-overexpressing control organoids or YAP-overexpressing organoids cultured in WRYTN (fig. S4, A and B). Collectively, several lines of evidence indicate that promoting YAP nuclear translocation increases human SGSPC potential.

Inhibition of MST1 and MST2 promotes the regeneration of salivary gland organoids after irradiation

The proximal-distal patterning that we observed for nuclear YAP (higher at the regeneration site and lower in distal areas) in ligated mouse salivary glands suggests that YAP nuclear activity is required during regeneration. Because YAP overexpression in human SGSPCs increased their self-renewal capacity, we investigated whether increased YAP nuclear activity could improve human salivary gland organoid response to irradiation. To increase YAP nuclear translocation upon radiation treatment, we treated human salivary gland organoids with XMU-MP-1, which is a potent inhibitor of MST1 and MST2 kinases and is known to promote liver regeneration after damage (*32*). Human SGSPC–derived organoids were seeded as single cells in Matrigel and exposed, at day 3 after seeding, to 2- or 4-gray (Gy) ionizing radiation; then, XMU-MP-1 or vehicle was added immediately after irradiation. XMU-MP-1–treated cells showed a higher OFE (Fig. 5A and fig. S5), thus reflecting a higher survival fraction of stem

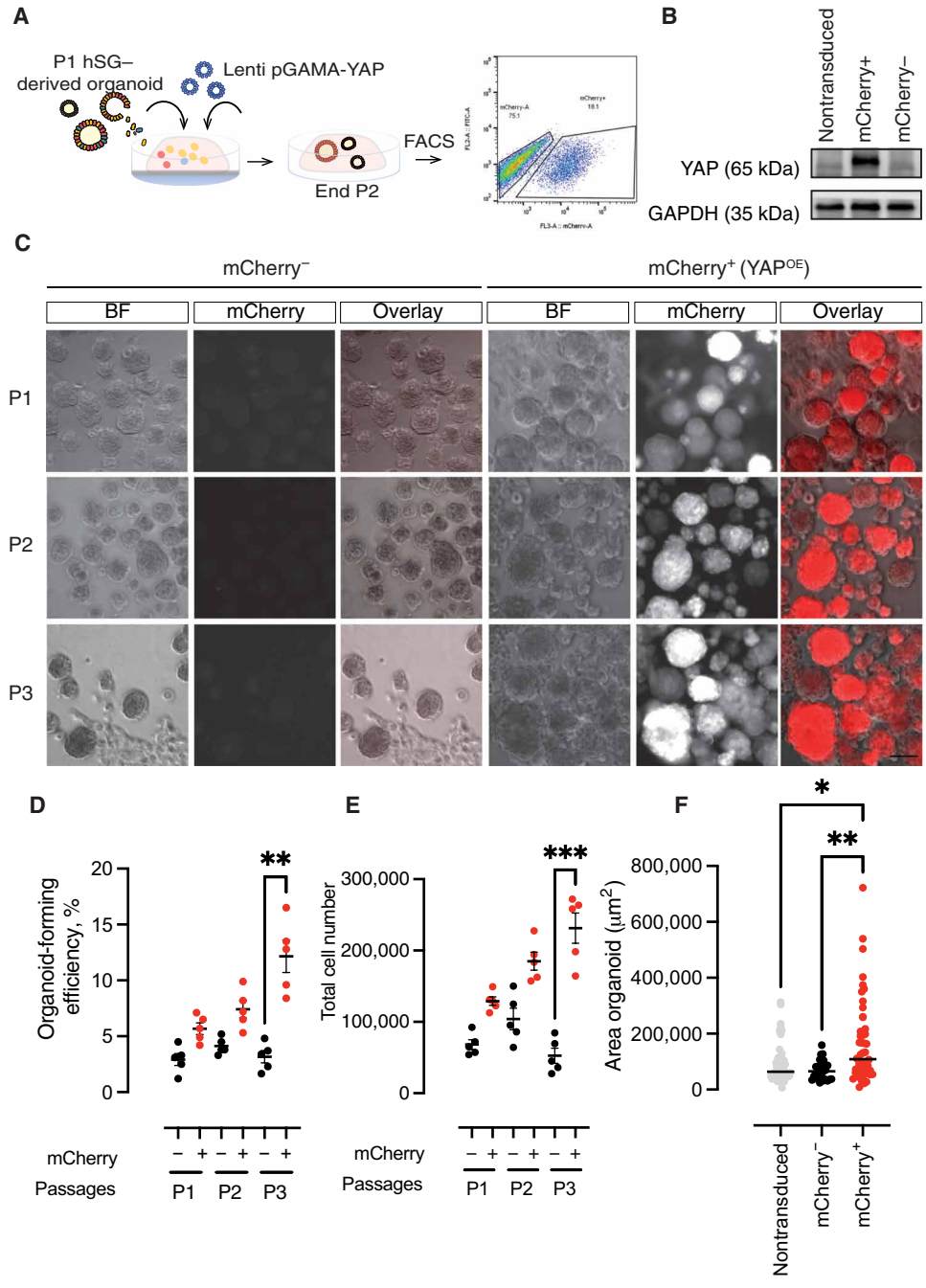

Fig. 4. YAP overexpression in human salivary gland–derived cells increases their self-renewal potential. (**A**) Schematic of the experiment performed on human salivary gland (hSG)–derived organoids that were dissociated and transfected with an mCherry-marked lentiviral vector encoding YAP (pGAMA-YAP). FACS plot shows the percentage of mCherry$^+$ cells indicating transduction efficiency. (**B**) Western blotting for YAP in lysates of secondary hSG organoids derived from cells that were not transduced or transduced with pGAMA-YAP. (**C**) Bright field (BF), mCherry and overlay, representative images; (**D**) organoid formation efficiency; (**E**) total cell numbers; and (**F**) size of primary (P1), secondary (P2), and tertiary (P3) hSG–derived organoids overexpressing YAP. Each dot represents a culture derived from a different patient. $n = 4$. Red dots, mCherry$^+$; black dots, mCherry$^-$. Data are represented as means ± SEM (D and E) and median (F). Statistical significance between groups was tested using Friedman test followed by Dunn's multiple comparison test (D and E) and by Kruskal-Wallis test followed by Dunn's multiple comparison test (F). *$P < 0.05$, **$P < 0.01$, and ***$P < 0.001$.

cells after treatment compared to cells that were irradiated but not treated with the drug. Cotreatment with XMU-MP-1 increased the amount of YAP in organoids derived from irradiated cells compared to organoids derived from cells that were only irradiated (Fig. 5, B and C). Organoids that were irradiated and treated with XMU-MP-1 were larger in size than irradiated-only organoids (Fig. 5, D to F), indicating that the induction of YAP nuclear activity after irradiation increased the proliferation of human SGSPCs and improved the response of human salivary gland organoids to radiation damage. These results indicate that our 3D organoid culture system can be used as a tool to study the underlying signaling pathways responsible for regeneration after radiation-induced damage. It also emphasizes the importance of YAP nuclear translocation as part of the Hippo signaling pathway during regeneration after damage.

DISCUSSION

After injury, stem and progenitor cells regenerate both the structural and functional units of the damaged tissue through a tightly controlled process that involves self-renewal and differentiation. Although it has been shown that transplantation of SGSPCs can rescue the secretory function of damaged salivary glands in mice (*26*, *27*, *33*, *34*), the mechanisms of regeneration after injury remain unclear. Here, we report that YAP activation is a critical step in the regeneration process of damaged adult salivary glands and that modulation of this pathway could be used to increase salivary gland stem cell potential. During homeostasis, salivary glands displayed low amounts of nuclear-localized YAP, which was confined to the acinar and intercalated ductal compartments known to be involved in the maintenance of the glands (*8*–*10*, *12*, *35*, *36*). After local injury, a marked and region-specific increase in nuclear YAP was observed at the regeneration site of ligated glands, supporting a role for inhibition of the Hippo signaling pathway in the response to damage.

YAP activation in the normally dormant excretory duct compartment of the salivary gland may point toward the existence of a "revival" cell, a cell that is nonregenerative during homeostasis

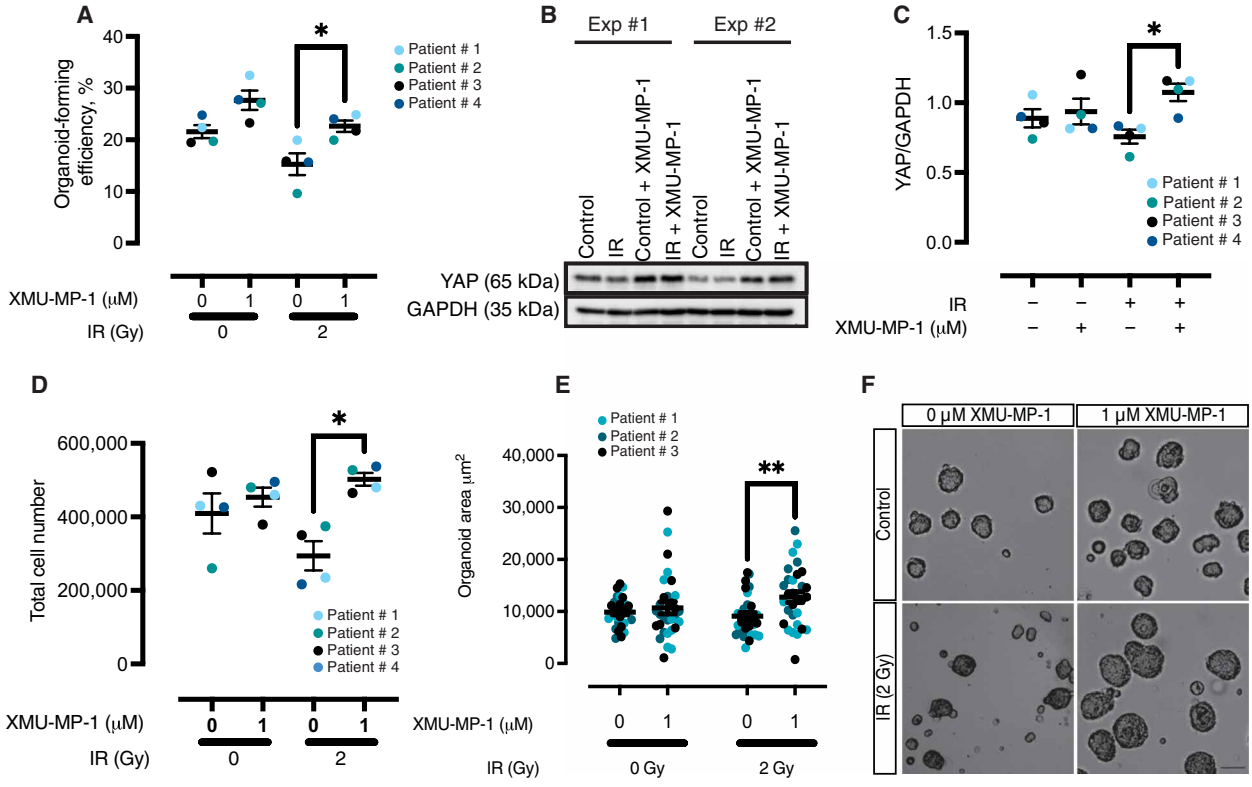

Fig. 5. Chemical inhibition of MST1 and MST2 improves salivary gland organoid formation after irradiation. (**A**) Organoid formation efficiency of single hSG-derived cells that were treated at day 3 with the MST1 and MST2 inhibitor XMU-MP-1 and ionizing radiation (IR) as indicated. (**B** and **C**) Representative Western blot analysis (B) and quantification (C) of YAP in lysates from hSG organoids that were untreated (control), irradiated (IR), treated with XMU-MP-1, or irradiated and treated with XMU-MP-1. The blot shows two experiments (exp #1 and exp #2) performed on cells from two different patients. (**D**) Total number of cells, (**E**) organoid size, and (**F**) representative images of organoids derived from hSGs that were treated as indicated. Scale bar, 50 μm. For all quantitative data, each color represents a culture derived from a different patient. $n = 4$ (A, C, and D) or $n = 3$ (E). Data are represented as means ± SEM. One-way ANOVA followed by Tukey's multiple comparison test was used to assess the difference between groups (A and C). Kruskal-Wallis test followed by Dunn's test for multiple comparison was used to test significance between groups (D). Two-way ANOVA (mixed model) followed by Sidak's test for multiple comparison was used to test the differences between the groups (E). *$P < 0.05$ and **$P < 0.01$.

but may, upon injury, switch to a stem-like cell state and drive the salivary gland regeneration program, similar to what has been recently described for smooth muscle actin–positive (SMA^+) and c-Kit^+ salivary gland cells (*37*). In line with this hypothesis, in the intestinal epithelium, certain rare $Clusterin^+$ cells, termed "revival stem cells", were shown to give rise to all major cell types of the intestine in a YAP-dependent manner (*38*). Although future in vivo work combining different injury models and lineage tracing will be fundamental to verifying the potential contribution of YAP-activated cells to acinar cell replacement, our in vitro data from organoid cultures of salivary gland–derived cells seem to support the regenerative potential of the striated and excretory ductal cell compartment.

Salivary gland–derived organoid cultures arise from $Epcam^+$ cells of the ductal epithelium (*26*). The competence of these cells to give rise to 3D structures (organoids) containing all major cell types spatially arranged similarly to the tissue of origin and to rescue hyposalivation upon intraglandular transplantation in mice (*26*) proves their potential in vitro plasticity and regenerative capacity. The in vivo observation that YAP is a key effector in salivary gland regeneration is supported by significant reductions in OFE and in the lobular organoid phenotype upon in vivo inhibition of YAP nuclear activity before cell harvesting and organoid formation.

Either promoting YAP nuclear translocation or overexpressing YAP resulted in a pronounced increase in the competence to form secondary and tertiary organoids, uncovering a role for YAP in the maintenance of stem/progenitor-like cells and self-renewal capacity. In agreement with what has been shown in intestinal organoids, it is tempting to speculate that salivary gland organoid development also follows a regenerative model that requires transient YAP activation (*28*). Contrary to what was shown in the intestine but in accordance with the in vivo role of YAP in embryonic salivary gland development (*25*), sustained YAP overexpression seems to promote the formation of branched organoids, whereas inhibition of YAP nuclear localization significantly reduces this phenotype, indicating a potential additional function of YAP in patterning and morphogenesis of human adult salivary gland epithelium. Although our observation highlights a role for YAP in directing the expansion and patterning of adult mouse and human salivary gland–derived epithelial cells, mapping the spatiotemporal activation of YAP and the other factors known to be involved during the regeneration process, such as Wnt (*26*) and autophagy (*39*), at the single-cell transcriptomic and proteomic levels will be required to unravel cell fate decisions and potential plasticity mechanisms of salivary gland cells. Further work, therefore, is needed to elucidate whether YAP could function

as a "gatekeeper" in the salivary gland, marking the boundary between the ductal compartment and the distal acinar compartment, similar to other branching organs (*40*–*42*).

We showed that our previously described in vitro model can be used to study the regeneration of salivary gland organoids after irradiation and that stimulating YAP nuclear translocation after irradiation significantly improved the radiation response of human salivary gland–derived cells. Moreover, transient chemical stimulation of YAP nuclear translocation could open new treatment possibilities to promote regeneration or enhance expansion of human SGSPCs in vitro for transplantation purposes. Our study supports the idea of YAP as a sensor of tissue integrity (*28*) and a key driver in regeneration of both murine and human salivary gland organoids; future studies should elucidate whether modulating YAP abundance or activity could induce in vivo regeneration, with the aim to use this approach as a regenerative therapy to ameliorate radiation-induced hyposalivation.

MATERIALS AND METHODS

Mice

Eight- to twelve-week-old female C57BL/6 mice were purchased from Envigo. Mice were housed in environmentally controlled rooms under conventional conditions and fed ad libitum in the Animal Facility of the University Medical Center Groningen. All experiments were performed according to approved institutional animal care and use committee protocols of the University of Groningen [under animal welfare body (IVD) protocol number 184824-01-001].

Patients

Human nonmalignant submandibular gland tissues were obtained from donors after informed consent and Institutional Review Board approval during an elective head and neck dissection procedure for the removal of squamous cell carcinoma of the oral cavity at the University Medical Center Groningen and Medical Center Leeuwarden.

Mouse submandibular gland ligation

C57BL/6 adult female mice were anesthetized with the use of isoflurane. A small incision was made in the neck to visualize the submandibular glands. Each submandibular gland was ligated with the use of (non-dissolvable) wire just below the sublingual gland, as previously published (*39*). Fourteen days later, the animals were re-anesthetized and sacrificed by cervical dislocation. Submandibular glands were isolated, ligation removed, and fixed in 4% formaldehyde overnight (ON) at room temperature (RT). Sections were used for IHC and immunofluorescence (as describe below) to determine the regenerative status of the gland. Control mice with matching sex and age were subjected to a mock ligation surgery that included isoflurane anesthesia, exposure of the submandibular gland, and suture of the incision.

To inhibit YAP nuclear activity, VP (100 mg/kg), dissolved in dimethyl sulfoxide (DMSO), was injected intraperitoneally at 3-day intervals until day 30 after ligation. Ligated and nonligated sham control mice were subjected to intraperitoneal injections of DMSO. At day 30, the animals were anesthetized and sacrificed by cervical dislocation and the gland was processed for organoids culture.

BrdU injection and labeling

To assess proliferation in the ligated submandibular gland and the control gland, mice were subjected to two intraperitoneal BrdU (Sigma-Aldrich, B5002-1G) injections. BrdU was dissolved in physiologic solution at a concentration of 50 mg/kg of body weight and injected 24 and 6 hours, respectively, before sacrifice. After BrdU labeling, IHC and quantification were performed as describe below.

IHC and immunofluorescence

All antibodies and reagents used in this study are listed in table S1. Tissues were isolated and fixed in 4% formaldehyde ON at RT. The tissues were then processed using an automatic tissue processor machine (Leica TP 1020) before standard paraffin embedding. Tissue blocks were sliced in 5-μm sections using a rotary microtome (Thermo Fisher Scientific, HM 340E).

For light microscopy, tissue sections were dewaxed before heat-activated antigen retrieval using a citric acid buffer containing 0.05% Tween 20 (10 mM, pH 6). Sections were allowed to cool down for 1 hour at RT followed by permeabilization on 0.4% Triton X-100 in phosphate-buffered saline (PBS). For BrdU staining, sections were treated with 2.5 M HCl for 25 min at RT and neutralized with 0.1 M sodium borate (pH 8.5) for 5 min. Sections were permeabilized in blocking solution [1% bovine serum albumin (BSA), 4% serum, and 0.4% Triton X-100 in PBS] and incubated with desired primary antibody ON at 4°C. The day after, sections were washed thoroughly and quenched in 0.5% H_2O_2 followed by secondary antibody incubation in blocking buffer (1% BSA, 4% donkey serum, and 0.4% Triton X-100 in PBS). VECTASTAIN ABC kit (Vector Labs) was used followed by 3.3′-diaminobenzide kit to detect positive staining. Last, sections were counterstained with hematoxylin, dehydrated, and coverslip-mounted using Eukit. Negative controls were generated by omitting the incubation with the primary antibody.

For fluorescence double labeling, heat-induced antigen retrieval and DNA denaturation procedure were performed as describe above. Tissue sections were incubated for 1 hour at RT in blocking buffer (1% BSA, 4% serum, and 0.4% Triton X-100 in PBS) before incubation in primary antibody solution ON at 4°C. The following day, sections were washed in PBS three times for 10 min each, followed by incubation in secondary antibody for 1 hour at RT. Last, slides were stained with 4′,6-diamidino-2-phenylindole,dihydrochloride (DAPI) and mounted using DAKO mounting media. The antibodies used and their final dilutions are as follows: rabbit anti-YAP1 (1:100; Cell Signaling Technology), rat anti-BrdU (1:100; Bio-Rad), and rabbit anti-AQP5 (1:200; Alomone).

Isolation of mouse and human submandibular gland cells

Submandibular glands were harvested from adult female mice, mechanically digested with the use of gentleMACS Dissociator (Miltenyi) and simultaneously digested in the digestion buffer containing collagenase type II (0,63 mg/ml; Gibco), hyaluronidase (0.5 mg/ml, Sigma-Aldrich), and $CaCl_2$ (6.25 mM; Sigma-Aldrich) in Hank's balanced salt solution (HBSS) containing 1% BSA (Invitrogen). The digestion procedure was repeated for two periods of 30 min in a shaking water bath at 37°C. To obtain optimal digestion, both submandibular glands from a single mouse were digested in a 2-ml volume of the digestion buffer. At the end of the digestion, cells were collected by centrifugation at 400*g* for 5 min and filtered through a 100-μm cell strainer (BD Biosciences). The resultant cell suspension was centrifuged at 400*g* for 5 min and resuspended in Dulbecco's modified Eagle's medium:F12 (DMEM/F12) containing penicillin-streptomycin antibiotics (Invitrogen), GlutaMAX, epidermal growth factor (EGF; 20 ng/ml; Sigma-Aldrich), fibroblast growth factor–2

(FGF2; 20 ng/ml; Sigma-Aldrich), N2 (Invitrogen), insulin (10 μg/ml; Sigma-Aldrich), and 1 μM dexamethasone (Sigma-Aldrich). Cells were plated at a density of 4×10^4 cells per well in a 12-well plate and incubated at 37°C and 5% CO_2 for 3 days as floating primary culture.

For human submandibular gland cell isolation, biopsies of non-malignant glands collected in the operating room were transferred to the laboratory in a 50-ml Falcon tube containing HBSS with 1% BSA on ice. The biopsy was weighted in a sterile petri dish and, using a sterile disposable scalpel, minced into small pieces. To obtain optimal digestion, 20 mg of tissue was processed per 1 ml of digestion buffer volume, with a maximum of 100 mg of tissue per tube. The human biopsies were then processed in the same manner as the mouse tissue.

Self-renewal assay of mouse and human salivary gland–derived cells

Three-day-old primary spheres were harvested and dispersed into single-cell suspension using 0.05% trypsin EDTA (Invitrogen). Single cells were counted and resuspended in culture media at a final concentration of 0.4×10^6 or 0.8×10^6 cells/ml. Cell suspension (25 μl) was mixed on ice with 50 μl of ice-cold Matrigel and the 75-μl gel pipetted in the middle of a 12-well plate. After solidifying the Matrigel, gels were covered in EM [DMEM/F12, penicillin-streptomycin (1×; Invitrogen), GlutaMAX (1×; Invitrogen), N2 (1×; Gibco), EGF (20 ng/ml; Sigma-Aldrich), FGF2 (20 ng/nl; Sigma-Aldrich), insulin (10 μg/ml; Sigma-Aldrich), dexamethasone (1 μM; Sigma-Aldrich), and Y27632 (10 μM; Sigma-Aldrich)] or WRYTN [DMEM/F12, penicillin-streptomycin (1×; Invitrogen), GlutaMAX (1×; Invitrogen), N2 (1×; Gibco), EGF (20 ng/ml; Sigma-Aldrich), FGF2 (20 ng/nl; Sigma-Aldrich), insulin (10 μg/ml; Sigma-Aldrich), dexamethasone (1 μM; Sigma-Aldrich), noggin (50 ng/ml; PeproTech-Bioconnect), A8301 (1 μM; Tocris), Y27632 (10 μM; Sigma-Aldrich), 10% R-spondin1–conditioned medium, and 50% Wnt3a-conditioned medium] media. To monitor the concentration of both Wnt3a and R-spondin in the conditioned media, we used the Dual-Luciferase Reporter Kit according to the manufacturer's protocol. Batches with a fold induction above 30 for the Wnt3 and above 5 for R-spondin were used to carry out experiments.

One week after seeding (end of the passage), the medium was replaced with Dispase enzyme (1 mg/ml in DMEM/F12 at 37°C for 30 to 45 min) to dissolve the gels. All the organoids released from the dissolved gels were processed into single cells using 0.05% trypsin-EDTA treatment to form single-cell suspension. Organoid and cell number at the end of the passage were noted, and the secondary organoid–derived single cells were reseeded in Matrigel to start a new passage. Number of organoids and single cells at the end of each passage were used to calculate OFE percentage (OFE%) and population doubling as follows

$$\text{Organoid formation efficiency (OFE\%)} = \frac{\text{Number of organoid harvested at the end of the passage}}{\text{Number of single cells seeded at the beginning of the passage}} \times 100$$

$$\text{Population doubling} = \frac{\ln(\text{harvestedcells}/\text{seededcells})}{\ln 2}$$

Irradiation treatment of mouse salivary gland–derived cells

Photon irradiation of 3-day-old salivary gland–derived organoids seeded in Matrigel was performed with ^{137}Cs source (IBL 637 Cesium-137 γ-ray machine) with a dose rate of 0.59 Gy/min.

Drug treatment of mouse and human salivary gland–derived cells

To inhibit or stimulate YAP activity during mouse salivary gland–derived organoid growth, cells were cultured in WRY [DMEM/F12, penicillin-streptomycin (1×; Invitrogen), GlutaMAX (1×; Invitrogen), N2 (1×; Gibco), EGF (20 ng/ml; Sigma-Aldrich), FGF2 (20 ng/nl; Sigma-Aldrich), insulin (10 μg/ml; Sigma-Aldrich), dexamethasone (1 μM; Sigma-Aldrich), Y27632 (10 μM; Sigma-Aldrich), 10% R-spondin1–conditioned medium, and 50% Wnt3a-conditioned medium]. For YAP nuclear activity inhibition, mouse organoids were cultured in WRY containing 5 or 20 μM VP. VP was added at day 0 or day 4 of culture, and media were refreshed every 2 days. The control group was cultured in WRY containing the same percentage of DMSO. To promote YAP nuclear translocation, LPA was added to mouse organoid culture at a final concentration of 10 or 100 μM from day 0. Medium was refreshed every 3 days.

To promote YAP nuclear translocation in human salivary gland–derived organoid culture, single cells were seeded in Matrigel and cultured in WRYTN media. Immediately after irradiation at day 3 after seeding, XMU-MP-1 was added to the wells at a final concentration of 1 or 3 μM. Medium was changed every 2 days.

siRNA transfection of mouse salivary gland–derived cells

Mouse salivary gland derived–cells were transfected using siGENOME SMARTpool siRNAYAP, siRNALATS1, and nontargeting siRNA from Dharmacon. Cells were seeded at a density of 1×10^5 to 1.5×10^5 in a 12-well plate and incubated at 37°C and 5% CO_2. After 1 day in culture, transfection was done using Lipofectamine 2000 (Invitrogen) in antibiotic-free medium according to the manufacturer's instructions. Five hours after transfection, medium was replaced with EM culture medium and cells were incubated at 37°C and 5% CO_2. A second round of transfection was performed, and 5 hours after transfection, cells were counted, resuspended in EM culture media at a density 0.8×10^6 cells/ml, and seeded in Matrigel. Seventy-two hours from the first transfection, cells were harvested to check knockdown efficiency. At the end of the passage, organoids and cells were counted to establish the OFE% and population doubling (as described above).

Lentiviral production

Human embryonic kidney 293T cells (1.5×10^6) were plated in poly-L-lysine–coated 10-cm dish in DMEM supplemented with 10% fetal bovine serum, penicillin-streptomycin (1×; Invitrogen), and GlutaMAX (1×; Invitrogen) and incubated ON at 37°C and 5% CO_2. On the next day, cells were transfected with 3 μg of p-GAMA YAP (Addgene) (*31*) or empty p-GAMA, 3 μg of the packaging plasmid PAX2, 0.7 μg of envelope plasmid vesicular stomatitis virus glycoprotein, and 40 μl of polyethylenimine (1 μg/ml) as previously described (*43*). On the following day, medium was changed to DMEM/F12. Two days after transfection, the viruses were collected, filtered through a sterile syringe filter with a 0.45-μm pore size and hydrophilic polyvinylidene difluoride (PVDF) membrane, and frozen in 250-μl aliquots at −80°C. We have titered the virus-containing supernatant by transduction of mCherry gene. Viruses were always in the range of 5.0×10^6 to 7.0×10^6 transduction unit/ml.

Lentiviral transduction and cell sorting of human salivary gland–derived cells

Human salivary gland–derived organoids at the end of P1 were released from Matrigel and dissociated into single cells using 0.05%

trypsin-EDTA (Invitrogen). Human salivary gland organoid–derived single cells were counted and resuspended in WRYTN media to a final concentration of 2.5×10^6 cells/ml. For each 100 µl of cell suspension, 250 µl of viral supernatant and polybrene (6 µg/ml) was added. The mixture was divided in 350-µl aliquots in a 24-well plate and incubated ON at 37°C and 5% CO_2. The day after transduction, single cells were counted to adjust for dead cells, resuspended in media to a final concentration of 0.8×10^6 cells/ml, and seeded in Matrigel into 12-well plates. The cells were cultured for 7 to 10 days in WRYTN media at 37°C and 5% CO_2. At day 7 (or day 10), Matrigel was dissolved with the use of Dispase enzyme (1 mg/ml) and organoids dispersed into single cells with the use of 0.05% trypsin-EDTA. Cells were washed with 0.2% BSA in PBS and resuspended in 0.2% BSA with the viability dye (DAPI) in PBS. YAP-overexpressing cells were isolated by FACS for mCherry-positive cells, seeded in Matrigel, and cultured in WRYTN for the next three passages.

Immunoblotting

To monitor endogenous gene responses, mouse and human organoids were harvested and centrifuged pellets were homogenized by sonication in 2× Laemmli buffer. Protein concentration of the lysates was determined using the Bradford quantification method. Homogenates were then boiled at 99°C for 5 min, and equal protein amounts were separated with 10 or 12% polyacrylamide gels and transferred to PVDF membranes using Trans-Blot Turbo System (Bio-Rad). The membranes were blocked in 5% BSA in PBS-Tween 20 and incubated for 1 hour at RT. Incubation with primary antibodies was done ON at 4°C followed by incubation with horseradish peroxidase–conjugated secondary antibodies. Membranes were developed using ECL reagent (Thermo Fisher Scientific), and the signal was detected using ChemiDoc imager (Bio-Rad). Densiometric analysis of Western blots at nonsaturated exposure was performed using ImageJ software, and the values were normalized against the one of glyceraldehyde-3-phosphate dehydrogenase (GAPDH) loading control. For immunoblots, the following primary antibodies at the indicated dilutions were used: rabbit anti-YAP (1:1000; Cell Signaling Technology), rabbit anti-LATS1 (1:1000; Cell Signaling Technology), and mouse anti-GAPDH (1:10000; Fitzgerald).

Quantification of IHC images

Light microscopy images, taken at 40×, were quantitatively analyzed for BrdU and YAP nuclear expression with the use of ImageJ (NIH) software. Five areas (309.68 µm by 232.26 µm) were chosen within each regenerative and homeostatic area of the ligated and control glands from three biological replicates ($n = 3$). For each replicate, three different sections were analyzed. To quantify the nuclear localization of BrdU or YAP, for each picture, positive nuclei were manually counted using ImageJ and the means of positive nuclei per square millimeter were calculated and plotted with the use of GraphPad Prism8.

Statistical analysis

All statistical analyses in this study were performed using GraphPad Prism8 software (GraphPad, La Jolla, CA, USA). The number of mice, patients, or individual organoids analyzed (n); presented error bars (SEM); statistical analysis used; and P values are all reported in each figure and/or figure legend.

SUPPLEMENTARY MATERIALS

www.science.org/doi/10.1126/scisignal.abk0599

Figs. S1 to S5
Table S1

View/request a protocol for this paper from *Bio-protocol*.

REFERENCES AND NOTES

1. R. L. Siegel, K. D. Miller, A. Jemal, Cancer statistics, 2018. *CA Cancer J. Clin.* **68**, 7–30 (2018).
2. A. Vissink, J. Jansma, F. K. Spijkervet, F. R. Burlage, R. P. Coppes, Oral sequelae of head and neck radiotherapy. *Crit. Rev. Oral Biol. Med.* **14**, 199–212 (2003).
3. O. Grundmann, G. C. Mitchell, K. H. Limesand, Sensitivity of salivary glands to radiation: From animal models to therapies. *J. Dent. Res.* **88**, 894–903 (2009).
4. G. C. Barnett, C. M. West, A. M. Dunning, R. M. Elliott, C. E. Coles, P. D. Pharoah, N. G. Burnet, Normal tissue reactions to radiotherapy: Towards tailoring treatment dose by genotype. *Nat. Rev. Cancer* **9**, 134–142 (2009).
5. C. Rocchi, E. Emmerson, Mouth-watering results: Clinical need, current approaches, and future directions for salivary gland regeneration. *Trends Mol. Med.* **26**, 649–669 (2020).
6. C. Metcalfe, N. M. Kljavin, R. Ybarra, F. J. de Sauvage, Lgr5+ stem cells are indispensable for radiation-induced intestinal regeneration. *Cell Stem Cell* **14**, 149–159 (2014).
7. A. W. Konings, R. P. Coppes, A. Vissink, On the mechanism of salivary gland radiosensitivity. *Int. J. Radiat. Oncol. Biol. Phys.* **62**, 1187–1194 (2005).
8. M. H. Aure, S. F. Konieczny, C. E. Ovitt, Salivary gland homeostasis is maintained through acinar cell self-duplication. *Dev. Cell* **33**, 231–237 (2015).
9. E. Emmerson, A. J. May, L. Berthoin, N. Cruz-Pacheco, S. Nathan, A. J. Mattingly, J. L. Chang, W. R. Ryan, A. D. Tward, S. M. Knox, Salivary glands regenerate after radiation injury through SOX2-mediated secretory cell replacement. *EMBO Mol. Med.* **10**, e8051 (2018).
10. A. J. May, N. Cruz-Pacheco, E. Emmerson, E. A. Gaylord, K. Seidel, S. Nathan, M. O. Muench, O. D. Klein, S. M. Knox, Diverse progenitor cells preserve salivary gland ductal architecture after radiation-induced damage. *Development* **145**, (2018).
11. B. Peter, M. A. Van Waarde, A. Vissink, E. J. 's-Gravenmade, A. W. Konings, Radiation-induced cell proliferation in the parotid and submandibular glands of the rat. *Radiat. Res.* **140**, 257–265 (1994).
12. M. Kimoto, Y. Yura, M. Kishino, S. Toyosawa, Y. Ogawa, Label-retaining cells in the rat submandibular gland. *J. Histochem. Cytochem.* **56**, 15–24 (2008).
13. L. Barazzuol, L. Ju, P. A. Jeggo, A coordinated DNA damage response promotes adult quiescent neural stem cell activation. *PLoS Biol.* **15**, e2001264 (2017).
14. G. Kalamakis, D. Brune, S. Ravichandran, J. Bolz, W. Fan, F. Ziebell, T. Stiehl, F. Catala-Martinez, J. Kupke, S. Zhao, E. Llorens-Bobadilla, K. Bauer, S. Limpert, B. Berger, U. Christen, P. Schmezer, J. P. Mallm, B. Berninger, S. Anders, A. Del Sol, A. Marciniak-Czochra, A. Martin-Villalba, Quiescence modulates stem cell maintenance and regenerative capacity in the aging brain. *Cell* **176**, 1407–1419.e14 (2019).
15. M. Kwak, N. Alston, S. Ghazizadeh, Identification of stem cells in the secretory complex of salivary glands. *J. Dent. Res.* **95**, 776–783 (2016).
16. P. L. Weng, M. H. Aure, T. Maruyama, C. E. Ovitt, Limited regeneration of adult salivary glands after severe injury involves cellular plasticity. *Cell Rep.* **24**, 1464–1470.e3 (2018).
17. C. A. Sullivan, R. I. Haddad, R. B. Tishler, A. Mahadevan, J. F. Krane, Chemoradiation-induced cell loss in human submandibular glands. *Laryngoscope* **115**, 958–964 (2005).
18. Y. Marmary, R. Adar, S. Gaska, A. Wygoda, A. Maly, J. Cohen, R. Eliashar, L. Mizrachi, C. Orfaig-Geva, B. J. Baum, S. Rose-John, E. Galun, J. H. Axelrod, Radiation-induced loss of salivary gland function is driven by cellular senescence and prevented by IL6 modulation. *Cancer Res.* **76**, 1170–1180 (2016).
19. P. van Luijk, S. Pringle, J. O. Deasy, V. V. Moiseenko, H. Faber, A. Hovan, M. Baanstra, H. P. van der Laan, R. G. Kierkels, A. van der Schaaf, M. J. Witjes, J. M. Schippers, S. Brandenburg, J. A. Langendijk, J. Wu, R. P. Coppes, Sparing the region of the salivary gland containing stem cells preserves saliva production after radiotherapy for head and neck cancer. *Sci. Transl. Med.* **7**, 305ra147 (2015).
20. R. Steenbakkers, M. I. van Rijn-Dekker, M. A. Stokman, R. G. J. Kierkels, A. van der Schaaf, J. G. M. van den Hoek, H. P. Bijl, M. C. A. Kramer, R. P. Coppes, J. A. Langendijk, P. van Luijk, Parotid gland stem cell sparing radiation therapy for patients with head and neck cancer: A double-blind randomized controlled trial. *Int. J. Radiat. Oncol. Biol. Phys.* S0360-3016(21)02827-3 (2021).
21. S. Yui, L. Azzolin, M. Maimets, M. T. Pedersen, R. P. Fordham, S. L. Hansen, H. L. Larsen, J. Guiu, M. R. P. Alves, C. F. Rundsten, J. V. Johansen, Y. Li, C. D. Madsen, T. Nakamura, M. Watanabe, O. H. Nielsen, P. J. Schweiger, S. Piccolo, K. B. Jensen, YAP/TAZ-dependent reprogramming of colonic epithelium links ECM remodeling to tissue regeneration. *Cell Stem Cell* **22**, 35–49 e37 (2018).
22. I. M. Moya, G. Halder, Hippo-YAP/TAZ signalling in organ regeneration and regenerative medicine. *Nat. Rev. Mol. Cell Biol.* **20**, 211–226 (2019).
23. T. Panciera, L. Azzolin, A. Fujimura, D. Di Biagio, C. Frasson, S. Bresolin, S. Soligo, G. Basso, S. Bicciato, A. Rosato, M. Cordenonsi, S. Piccolo, Induction of expandable tissue-specific stem/progenitor cells through transient expression of YAP/TAZ. *Cell Stem Cell* **19**, 725–737 (2016).

24. A. Gregorieff, Y. Liu, M. R. Inanlou, Y. Khomchuk, J. L. Wrana, Yap-dependent reprogramming of Lgr5(+) stem cells drives intestinal regeneration and cancer. *Nature* **526**, 715–718 (2015).
25. A. D. Szymaniak, R. Mi, S. E. McCarthy, A. C. Gower, T. L. Reynolds, M. Mingueneau, M. Kukuruzinska, X. Varelas, The Hippo pathway effector YAP is an essential regulator of ductal progenitor patterning in the mouse submandibular gland. *eLife* **6**, e23499 (2017).
26. M. Maimets, C. Rocchi, R. Bron, S. Pringle, J. Kuipers, B. N. Giepmans, R. G. Vries, H. Clevers, G. de Haan, R. van Os, R. P. Coppes, Long-term in vitro expansion of salivary gland stem cells driven by wnt signals. *Stem Cell Rep.* **6**, 150–162 (2016).
27. L. S. Nanduri, M. Baanstra, H. Faber, C. Rocchi, E. Zwart, G. de Haan, R. van Os, R. P. Coppes, Purification and ex vivo expansion of fully functional salivary gland stem cells. *Stem Cell Rep.* **3**, 957–964 (2014).
28. D. Serra, U. Mayr, A. Boni, I. Lukonin, M. Rempfler, L. Challet Meylan, M. B. Stadler, P. Strnad, P. Papasaikas, D. Vischi, A. Waldt, G. Roma, P. Liberali, Self-organization and symmetry breaking in intestinal organoid development. *Nature* **569**, 66–72 (2019).
29. S. Pringle, R. Van Os, R. P. Coppes, Concise review: Adult salivary gland stem cells and a potential therapy for xerostomia. *Stem Cells* **31**, 613–619 (2013).
30. F. X. Yu, B. Zhao, N. Panupinthu, J. L. Jewell, I. Lian, L. H. Wang, J. Zhao, H. Yuan, K. Tumaneng, H. Li, X. D. Fu, G. B. Mills, K. L. Guan, Regulation of the Hippo-YAP pathway by G-protein-coupled receptor signaling. *Cell* **150**, 780–791 (2012).
31. H. Qin, M. Hejna, Y. Liu, M. Percharde, M. Wossidlo, L. Blouin, J. Durruthy-Durruthy, P. Wong, Z. Qi, J. Yu, L. S. Qi, V. Sebastiano, J. S. Song, M. Ramalho-Santos, YAP Induces Human Naive Pluripotency. *Cell Rep.* **14**, 2301–2312 (2016).
32. F. Fan, Z. He, L. L. Kong, Q. Chen, Q. Yuan, S. Zhang, J. Ye, H. Liu, X. Sun, J. Geng, L. Yuan, L. Hong, C. Xiao, W. Zhang, X. Sun, Y. Li, P. Wang, L. Huang, X. Wu, Z. Ji, Q. Wu, N. S. Xia, N. S. Gray, L. Chen, C. H. Yun, X. Deng, D. Zhou, Pharmacological targeting of kinases MST1 and MST2 augments tissue repair and regeneration. *Sci. Transl. Med.* **8**, 352ra108 (2016).
33. L. S. Nanduri, I. M. Lombaert, M. van der Zwaag, H. Faber, J. F. Brunsting, R. P. van Os, R. P. Coppes, Salisphere derived c-Kit+ cell transplantation restores tissue homeostasis in irradiated salivary gland. *Radiother. Oncol.* **108**, 458–463 (2013).
34. S. Pringle, M. Maimets, M. van der Zwaag, M. A. Stokman, D. van Gosliga, E. Zwart, M. J. Witjes, G. de Haan, R. van Os, R. P. Coppes, Human salivary gland stem cells functionally restore radiation damaged salivary glands. *Stem Cells* **34**, 640–652 (2016).
35. Y. J. Kim, H. J. Kwon, N. Shinozaki, S. Hashimoto, M. Shimono, S. W. Cho, H. S. Jung, Comparative analysis of ABCG2-expressing and label-retaining cells in mouse submandibular gland. *Cell Tissue Res.* **334**, 47–53 (2008).
36. A. M. Chibly, L. Querin, Z. Harris, K. H. Limesand, Label-retaining cells in the adult murine salivary glands possess characteristics of adult progenitor cells. *PLOS ONE* **9**, e107893 (2014).
37. N. Ninche, M. Kwak, S. Ghazizadeh, Diverse epithelial cell populations contribute to the regeneration of secretory units in injured salivary glands. *Development* **147**, dev192807 (2020).
38. A. Ayyaz, S. Kumar, B. Sangiorgi, B. Ghoshal, J. Gosio, S. Ouladan, M. Fink, S. Barutcu, D. Trcka, J. Shen, K. Chan, J. L. Wrana, A. Gregorieff, Single-cell transcriptomes of the regenerating intestine reveal a revival stem cell. *Nature* **569**, 121–125 (2019).
39. I. Orhon, C. Rocchi, B. Villarejo-Zori, P. Serrano Martinez, M. Baanstra, U. Brouwer, P. Boya, R. Coppes, F. Reggiori, Autophagy induction during stem cell activation plays a key role in salivary gland self-renewal. *Autophagy* **2021**, 1–16 (2021).
40. J. E. Mahoney, M. Mori, A. D. Szymaniak, X. Varelas, W. V. Cardoso, The hippo pathway effector Yap controls patterning and differentiation of airway epithelial progenitors. *Dev. Cell* **30**, 137–150 (2014).
41. A. Mamidi, C. Prawiro, P. A. Seymour, K. H. de Lichtenberg, A. Jackson, P. Serup, H. Semb, Mechanosignalling via integrins directs fate decisions of pancreatic progenitors. *Nature* **564**, 114–118 (2018).
42. E. A. Rosado-Olivieri, K. Anderson, J. H. Kenty, D. A. Melton, YAP inhibition enhances the differentiation of functional stem cell-derived insulin-producing β cells. *Nat. Commun.* **10**, 1464 (2019).
43. H. Schepers, D. van Gosliga, A. T. Wierenga, B. J. Eggen, J. J. Schuringa, E. Vellenga, STAT5 is required for long-term maintenance of normal and leukemic human stem/progenitor cells. *Blood* **110**, 2880–2888 (2007).

Acknowledgments: We would like to thank the maxillofacial surgical team of the University Medical Center Groningen and Medical Center Leeuwarden for providing donor biopsies and M. Stokman for coordination of the sampling of donor material. We also thank the staff members of the Department of Biomedical Sciences of Cells and Systems of the University Medical Center of Groningen for fruitful discussion of data. **Funding:** This work was supported by grants from KWF Kankerbestrijding (RUG 2013-5792 and 12092 to R.P.C.). **Author contributions:** C.R. conceptualized the study, designed and performed the experiments, analyzed and interpreted data, and wrote and edited the paper. D.C. contributed to the animal in vivo experiment as well as to the in vitro experiments. P.S.M. and U.B. contributed to the animal ligation experiments. A.J.-d.B. and M.B. contributed to the mouse and human in vitro experiments (culture and FACS). C.d.A.Z. contributed to the mouse in vitro experiments. H.S. contributed to the conceptualization of the lentiviral experiments, interpretation of the data, and manuscript writing. R.v.O. and L.B. contributed to the conceptualization, data analysis and interpretation, the design, and manuscript writing. R.P.C. provided financial support and contributed to the conceptualization, data analysis and interpretation, the design, and manuscript writing. **Competing interests:** The authors declare that they have no competing interests. **Data and materials availability:** All data needed to evaluate the conclusions in the paper are present in the paper or the Supplementary Materials. Further information and requests for resources and reagents should be directed to and will be fulfilled by the corresponding authors, L.B. (l.barazzuol@umcg.nl) and R.P.C. (r.p.coppes@umcg.nl).

Submitted 18 June 2021
Accepted 3 November 2021
Published 7 December 2021
10.1126/scisignal.abk0599

Science Signaling

The Hippo signaling pathway effector YAP promotes salivary gland regeneration after injury

Cecilia RocchiDavide CinatPaola Serrano MartinezAnne L. Jellema-de BruinMirjam BaanstraUilke BrouwerCinthya del Angel ZuivreHein SchepersRonald van OsLara BarazzuolRobert P. Coppes

Sci. Signal., 14 (712), eabk0599. • DOI: 10.1126/scisignal.abk0599

Yap for regenerating salivary glands

Radiotherapy for head and neck cancers often damages the salivary glands, resulting in potentially permanent xerostomia (dry mouth). The mitotically active acinar cells of the salivary gland secretory compartment have some regenerative capacity, but sparing the main ducts from irradiation preserves regeneration. Rocchi *et al.* showed that surgically induced injury of salivary glands in mice stimulated proliferation of ductal cells, which showed nuclear accumulation of the transcriptional coactivator YAP. Activating YAP in cells from injured mouse glands or in irradiated human primary salivary gland cells enhanced organoid formation and promoted organoid branching. These findings demonstrate the regenerative potential of ductal cells and suggest that stimulating YAP activity might be exploited to promote salivary gland regeneration after injury.

Science Signaling (ISSN) is published by the American Association for the Advancement of Science. 1200 New York Avenue NW, Washington, DC 20005. The title *Science Signaling* is a registered trademark of AAAS.